



High frame rate synthetic aperture duplex imaging

Stuart, Matthias Bo; Tomov, Borislav Gueorguiev; Pihl, Michael Johannes; Jensen, Jørgen Arendt

Published in:
Proceedings of IEEE International Ultrasonic Symposium

Link to article, DOI:
[10.1109/ULTSYM.2013.0161](https://doi.org/10.1109/ULTSYM.2013.0161)

Publication date:
2013

[Link back to DTU Orbit](#)

Citation (APA):
Stuart, M. B., Tomov, B. G., Pihl, M. J., & Jensen, J. A. (2013). High frame rate synthetic aperture duplex imaging. In *Proceedings of IEEE International Ultrasonic Symposium* (pp. 623 - 626). IEEE.
<https://doi.org/10.1109/ULTSYM.2013.0161>

General rights

Copyright and moral rights for the publications made accessible in the public portal are retained by the authors and/or other copyright owners and it is a condition of accessing publications that users recognise and abide by the legal requirements associated with these rights.

- Users may download and print one copy of any publication from the public portal for the purpose of private study or research.
- You may not further distribute the material or use it for any profit-making activity or commercial gain
- You may freely distribute the URL identifying the publication in the public portal

If you believe that this document breaches copyright please contact us providing details, and we will remove access to the work immediately and investigate your claim.

High Frame Rate Synthetic Aperture Duplex Imaging

Matthias Bo Stuart, Borislav Gueorguiev Tomov, Michael Johannes Pihl, and Jørgen Arendt Jensen
Center for Fast Ultrasound Imaging, Department of Electrical Engineering, Technical University of Denmark

Abstract—Conventional color flow images are limited in velocity range and can either show the high velocities in systole or be optimized for the lower diastolic velocities. The full dynamics of the flow is, thus, hard to visualize. The dynamic range can be significantly increased by employing synthetic aperture flow imaging as demonstrated in this paper. Synthetic aperture, directional beamforming, and cross-correlation are used to produce B-mode and vector velocity images at high frame rates. The frame rate equals the effective pulse repetition frequency of each imaging mode. Emissions for making the B-mode images and velocity maps are interleaved in a 1-to-1 ratio. This provides continuous data allowing a wide range of velocities to be estimated. Two cases are considered in the flow estimation: In the first case, the angle of the flow is determined from the B-mode image. In the other case, the angle is determined by estimating the flow velocity in all directions and choosing the one with the strongest correlation. The method works for all angles, including fully axial and fully transverse flows. Field II simulations with a 192 element, 7 MHz linear array are made of laminar, transverse flow profiles. For a simulated peak velocity of 0.5 m/s, the relative bias is -6.8% and the relative standard deviation is 6.1% . The bias on the angle is 0.98 degrees with a standard deviation of 2.39 degrees when using the flow estimator to determine the angle. For a peak velocity of 0.05 m/s, the relative bias of the velocity estimation is -1.8% and the relative standard deviation 5.4% . The approach can thus estimate both high and low velocities with equal accuracy and thereby makes it possible to present vector flow images with a high dynamic range. Measurements are made using the SARUS research scanner, a linear array transducer similar to the simulated one, and a recirculating flow rig with a blood mimicking fluid and a parabolic flow profile with a peak velocity of approximately 0.3 m/s. The relative bias of the velocity estimation is 0.19% and the mean relative standard deviation 4.9% . For the direction estimation, the bias is 3.2 degrees with a standard deviation of 1.6 degrees.

I. INTRODUCTION

Ultrasound imaging of blood velocities is a well-established tool for diagnosing cardiovascular diseases. There are multiple approaches to detecting the velocities [1], and this paper focuses on the time-shift based estimator [2], also known as the cross-correlation estimator.

A typical color flow image is shown in Fig. 1(a) for the carotid at peak systole. The image is acquired by repeatedly pulsing in the same direction 8 times and then finding the velocity in that direction. The sequence is then repeated over the imaging region. The pulse repetition frequency is adjusted to match the peak velocity in the vessel, so that no aliasing occurs and the complete vessel is filled out during systole. The corresponding image at diastole is seen in Fig. 1(b), which is taken right before the image in Fig. 1(a). Here there is hardly any flow in vessel, which obviously is not true for the carotid artery. The reason is that the velocities are significantly lower and are difficult to detect for the system. The minimum detectable velocity v_{min} for the estimator roughly corresponds

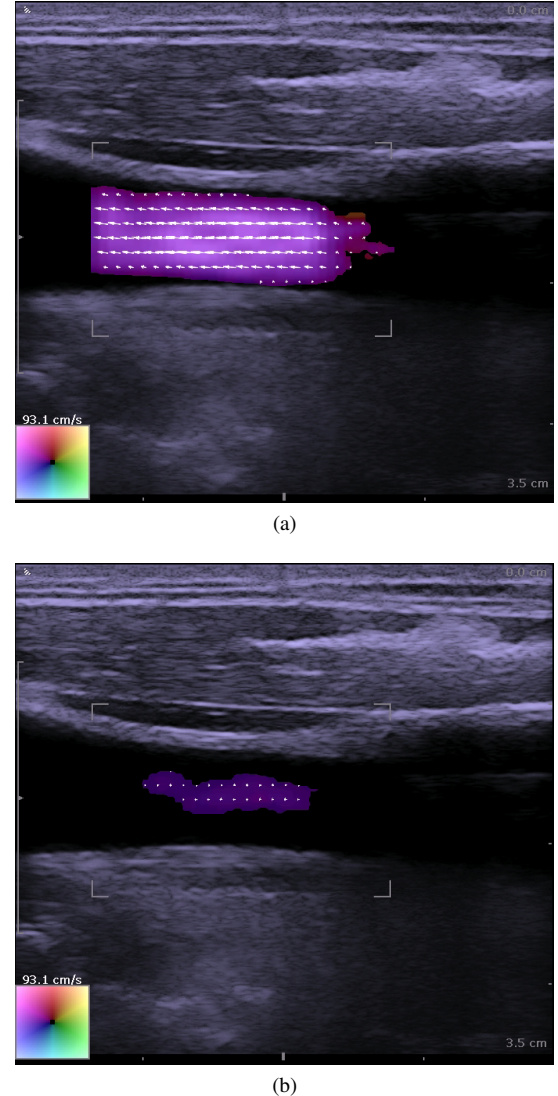


Fig. 1. Vector flow images of the carotid artery at peak systole and end diastole.

to:

$$v_{min} = \frac{v_{max}}{N}, \quad (1)$$

where N is the number of emissions in one direction and v_{max} is the maximum detectable velocity given by

$$v_{max} = \frac{f_{prf}}{f_0} \frac{c}{4}. \quad (2)$$

Here c is the speed of sound, f_0 is the emitted frequency and f_{prf} is the pulse repetition frequency. f_{prf} can then be adjusted to estimate lower velocities, but this will introduce aliasing during systole. Another solution is to increase N , but

this will correspondingly reduce the frame rate. The scheme is, thus, limited by the dynamic range of the velocity estimation, which stems from the sequential acquisition of the data.

Synthetic aperture imaging can solve the dynamic range problem. In synthetic aperture imaging, an image of the entire insonified region is created at each emission [3], [4]. Each of these images is referred to as low-resolution image. By summing all low-resolution images in an emission sequence, a high-resolution image is formed. If the emission sequence is repeating with no break between the last emission of one iteration of the sequence and the first emission of the next iteration, data will be continuously available. In this case, recursive synthetic aperture (RSA) imaging is possible [5]. In RSA imaging, the low-resolution image contribution from a given emission is replaced when that emission is repeated. In this way, new high-resolution images can be created at the rate of the pulse repetition frequency (PRF).

RSA imaging can be applied to blood flow imaging when using cross-correlation estimators [6]. Combined with directional beamforming, both the velocity and angle of the flow can be determined. The concept is similar to that used to compensate for tissue motion in synthetic aperture B-mode imaging [7]. Here, a duplex imaging sequence is created that provides continuous data for both B-mode and flow imaging.

This paper combines RSA, directional beamforming, and synthetic aperture duplex imaging to produce high-quality anatomical images and vector velocity estimates with high dynamic range and high frame rate.

II. METHODS

This section presents the flow estimation method. It is similar to a previously presented method used for tissue motion compensation in synthetic aperture anatomical imaging [7].

Two emission sequences are needed for duplex imaging: one for B-mode images and one for flow estimation. The length of the B-mode sequence is N_B emissions, while the length of the flow sequence is N_F emissions. To provide continuous data, these sequences are interleaved in a 1-to-1 ratio. When the last emission is reached in one of the sequences, that sequence is simply restarted while the other sequence continues without interruption. In this way, an infinitely repeating emission sequence is produced for both imaging modes.

Denoting the pulse repetition frequency (PRF) of the combined sequences f_{prf} , the effective PRF of either imaging mode (B-mode or flow) is $f_{prf}/2$.

The acquired data from the B-mode emissions are used to create RSA B-mode images. This method produces high-resolution images at a frame rate equaling the effective PRF.

For the flow processing, directional beamforming and RSA imaging are used. For each point in which the blood flow is to be estimated, lines are beamformed in the direction of the flow. If the flow estimator is used to determine the angle of the flow, lines are beamformed in all radial directions instead. This is done for every image point and every emission. The lines from N_F successive emissions are summed to form a high resolution flow image. Stationary echo cancelling is performed by subtracting the average of a moving window of

N_{ec} high resolution images from each high resolution image. The lines in high resolution images spaced N_F images are then correlated. The flow velocity is then determined by the lag of the peak of the correlation by

$$v = \frac{d_r l}{N_B f_{prf}} \quad (3)$$

where d_r is the sample distance along the beamformed line and l is the lag. When also determining the angle, the maximum is taken across all the correlation functions for a given point.

III. EXPERIMENTAL SETUP

Circular symmetric parabolic flow profiles are simulated using Field II [8], [9]. A 7 MHz, 192 element, lambda-pitch, linear array transducer is used with defocused emissions. A 2-cycle sinusoidal pulse with a center frequency of 7 MHz is used. The simulated vessel has a diameter of 1 cm and is parallel to the transducer surface. Two peak velocities are simulated: 0.05 m/s and 0.50 m/s.

Measurements are made using the SARUS research scanner [10], and a commercial linear array transducer (BK8804, BK Medical, Herlev, Denmark). Here, focused emissions are used to increase the energy of the returned signal. Otherwise, the parameters of the image acquisition and processing are as for the simulations. Scans are made on a recirculating flow rig with laminar flow and a peak velocity of 0.30 m/s. Approximately 0.2 seconds of data have been acquired at a flow-to-beam angle of approximately 90 degrees, i.e., fully transverse flow.

The flow rig includes a magnetometer (Magflo MAG3000 by Danfoss, Nordborg, Denmark) that measures the flow rate. The flow rig has a long entrance length and a constant flow, such that a parabolic flow profile can be assumed. From the flow rate and the radius of the vessel, the peak velocity can be calculated and used as a reference.

RF data are recorded for all channels individually in receive. These data are then processed offline using a beamformation toolbox developed in-house (BFT3) [11].

IV. RESULTS

Fig. 2 shows the simulation results for $v_{peak} = 0.5\text{m/s}$. The top graph shows the estimated velocity profile along the vessel plus/minus one standard deviation. The middle graph shows the estimated angle plus/minus one standard deviation when radial lines are beamformed at every 10 degrees. The lower graph shows the velocity profile in the direction of the estimated angle. Fig. 3 shows the simulation results for $v_{peak} = 0.05\text{m/s}$ in the same order as Fig. 2.

Fig. 4 shows a flow profile plus/minus one standard deviation for the measurement. For the velocity magnitude, the solid line indicates the estimated velocity, while the dashed lines indicate plus/minus one standard deviation.

Table I shows the bias and standard deviations of the simulations and the measurement. For the velocity magnitudes, the relative bias and the mean relative standard deviations are shown. For the velocity directions, the bias and standard deviations are shown. For the measurements, a parabolic profile with $v_{peak} = 0.3\text{m/s}$ is fitted to the data and used as the true velocity profile.

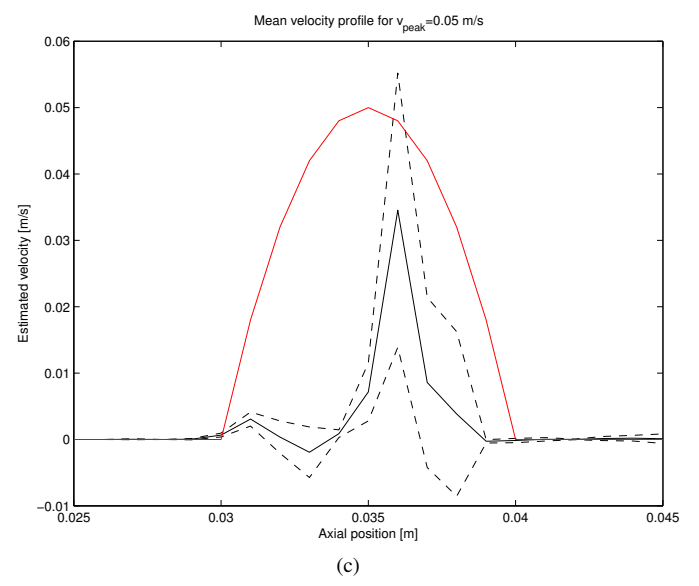
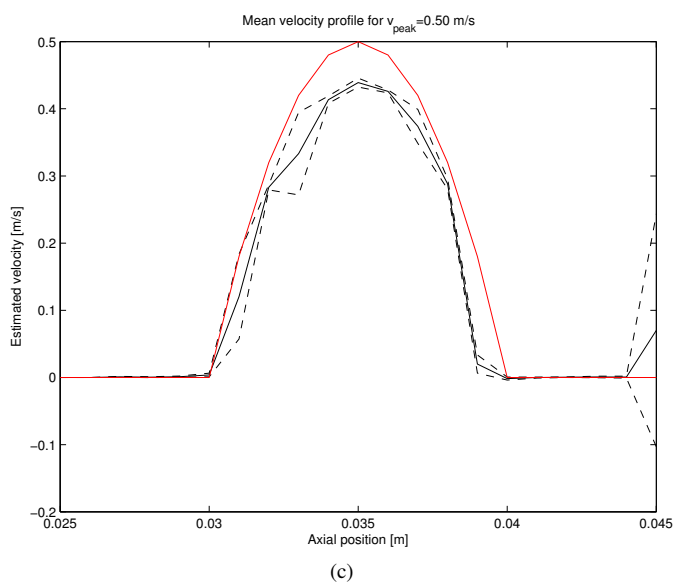
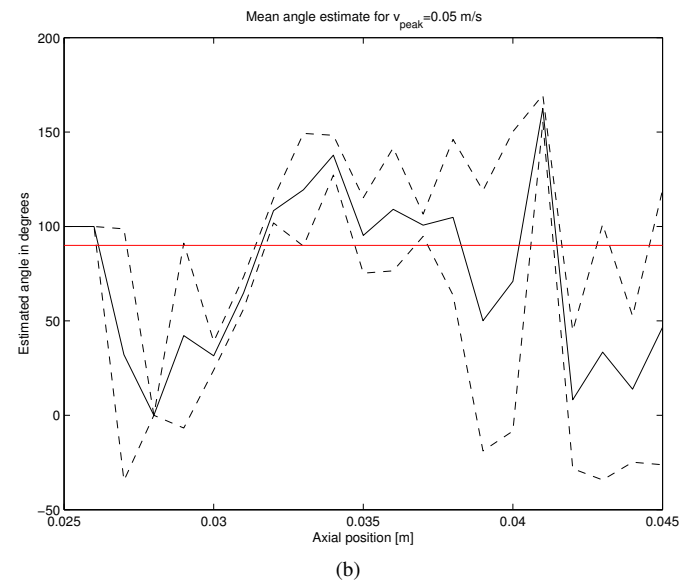
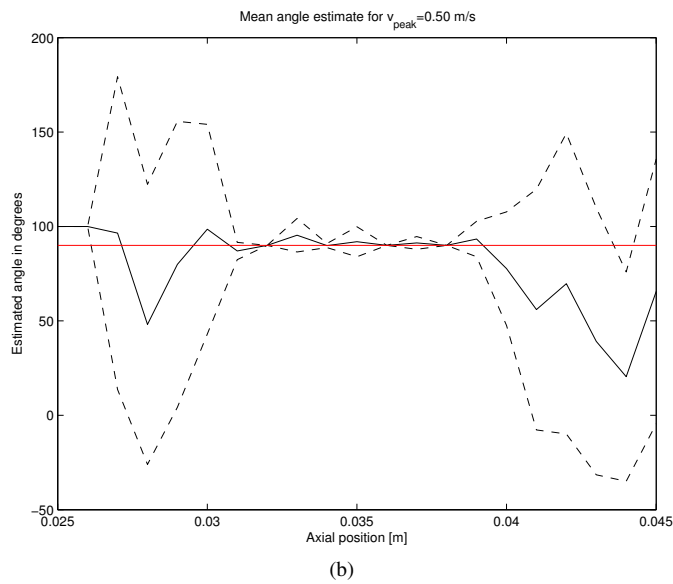
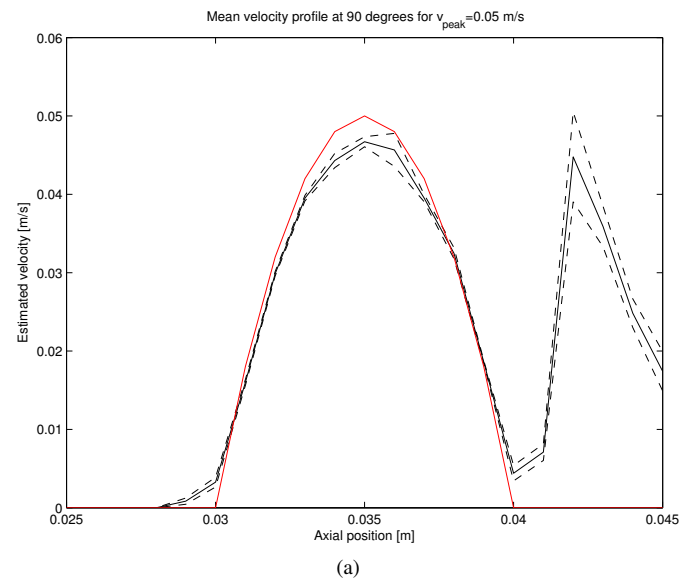
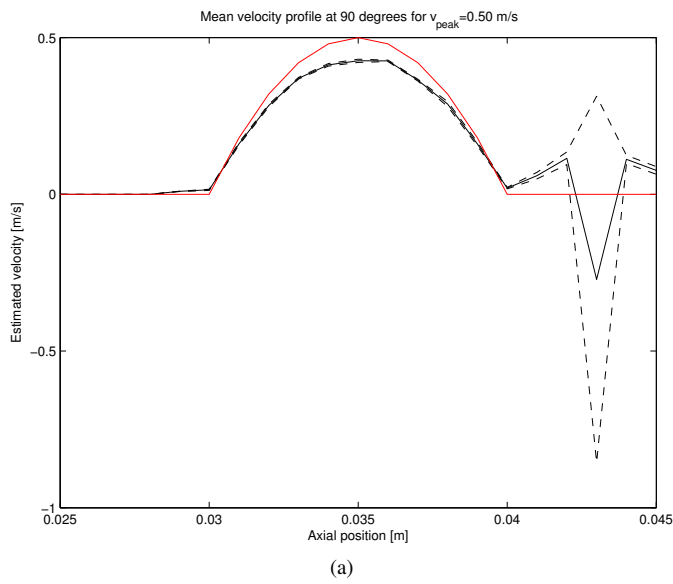


Fig. 2. Flow estimates from simulated data with a peak velocity of 0.5 m/s.

Fig. 3. Flow estimates from simulated data with a peak velocity of 0.05 m/s.

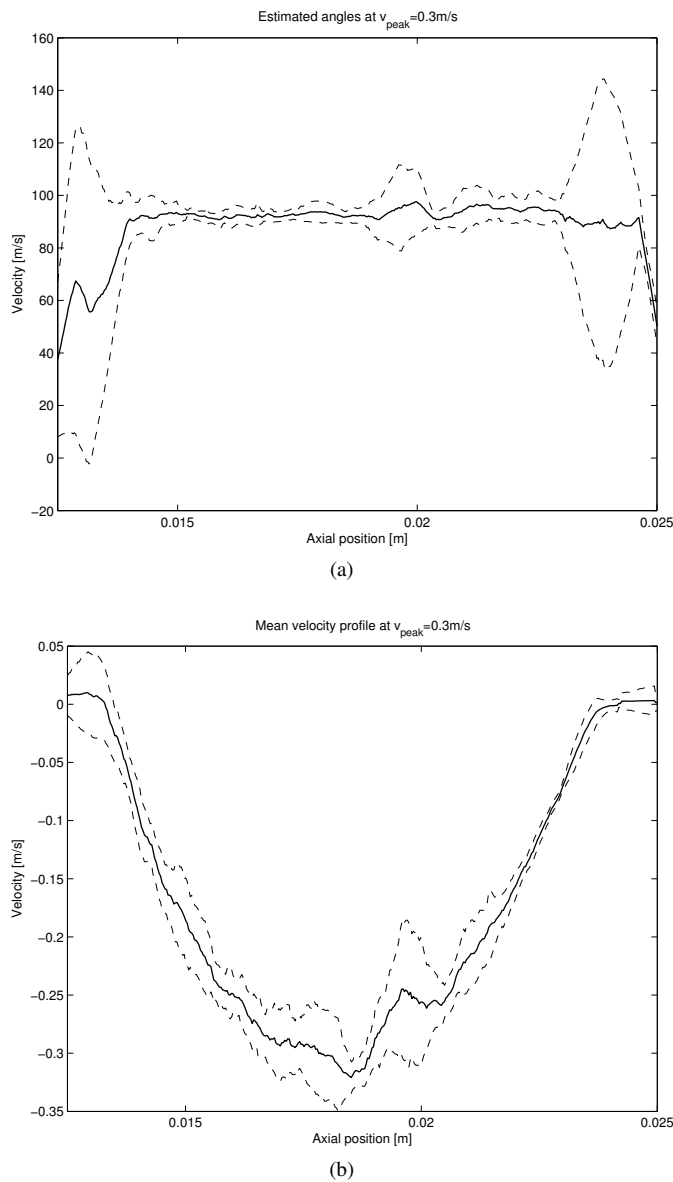


Fig. 4. Flow estimates in the flow rig at 90 degrees: (a) shows the velocity direction, while (b) shows the velocity magnitude.

TABLE I. THE BIAS AND STANDARD DEVIATIONS OF SIMULATED AND MEASURED VELOCITY ESTIMATES.

	Velocity	Angle	Velocity at detected angle
	%	Degrees	%
Sim, $v = 0.05 \text{ m/s}$	(-1.8, 5.4)	(8.9, 26.7)	(-49.7, 33.7)
Sim, $v = 0.50 \text{ m/s}$	(-6.8, 6.1)	(0.98, 2.39)	(-10.9, 8.8)
Measurement	-	(3.2, 1.6)	(0.19, 4.9)

As can be seen, the velocity profile is accurately determined. For the slowly moving flow, the angle is not determined correctly, due to the very small movement (a fraction of the wavelength) between emissions. However, given the proper flow direction, the proposed method gives accurate results for both high and low velocities.

V. DISCUSSION

Given the accuracy of the proposed method, it can be used to expand the dynamic range of detectable flow velocities.

While an upper limit remains, it can be increased by increasing the pulse repetition frequency and/or lowering the length of the flow estimation emission sequence. Regardless of these parameters, having continuously available data removes any theoretical limit on the lower limit of the detectable velocities.

In this way, the issue demonstrated in Fig. 1 can be efficiently solved by setting the pulse repetition frequency such that the velocities at peak systole can be estimated. Then the velocities are detectable across the entire cardiac cycle without further operator adjustments. Furthermore, given the availability of continuous data, the image can be updated with every new emission, essentially producing a frame rate equal to that of the pulse repetition frequency.

VI. CONCLUSIONS

A synthetic aperture duplex imaging sequence for B-mode and flow imaging has been presented. The flow processing has been evaluated through simulations and measurements. The proposed method successfully estimates the flow profile in all cases and the direction of the flow in most cases. The method can reduce the operator dependence on flow imaging by expanding the range of detectable velocities, while providing a frame rate equal to that of the PRF.

ACKNOWLEDGEMENT

This work was supported by grant 024-2008-3 and grant 82-2012-4 from the Danish Advanced Technology Foundation and by B-K Medical Aps.

REFERENCES

- [1] J. A. Jensen, *Estimation of Blood Velocities Using Ultrasound: A Signal Processing Approach*. New York: Cambridge University Press, 1996.
- [2] D. Dotti, E. Gatti, V. Svelto, A. Uggè, and P. Vidali, "Blood flow measurements by ultrasound correlation techniques," *Energia Nucleare*, vol. 23, pp. 571-575, 1976.
- [3] M. Soumekh, *Synthetic aperture radar. Signal processing with MATLAB algorithms*. New York: John Wiley & Sons, Inc., 1999.
- [4] J. J. Flaherty, K. R. Erikson, and V. M. Lund, "Synthetic aperture ultrasound imaging systems," United States Patent, US 3,548,642, 1967, United States Patent, US 3,548,642, 1967, Published 22 Dec 1970.
- [5] S. I. Nikolov, K. Gammelmark, and J. A. Jensen, "Recursive ultrasound imaging," in *Proc. IEEE Ultrason. Symp.*, vol. 2, 1999, pp. 1621-1625.
- [6] J. A. Jensen and S. I. Nikolov, "Directional synthetic aperture flow imaging," *IEEE Trans. Ultrason., Ferroelec., Freq. Contr.*, vol. 51, pp. 1107-1118, 2004.
- [7] K. L. Gammelmark and J. A. Jensen, "Duplex synthetic aperture imaging with tissue motion compensation," in *Proc. IEEE Ultrason. Symp.*, 2003, pp. 1569-1573.
- [8] J. A. Jensen, "Field: A program for simulating ultrasound systems," *Med. Biol. Eng. Comp.*, vol. 10th Nordic-Baltic Conference on Biomedical Imaging, Vol. 4, Supplement 1, Part 1, pp. 351-353, 1996.
- [9] J. A. Jensen and N. B. Svendsen, "Calculation of Pressure Fields from Arbitrarily Shaped, Apodized, and Excited Ultrasound Transducers," *IEEE Trans. Ultrason., Ferroelec., Freq. Contr.*, vol. 39, pp. 262-267, 1992.
- [10] J. A. Jensen, H. Holten-Lund, R. T. Nilsson, M. Hansen, U. D. Larsen, R. P. Domsten, B. G. Tomov, M. B. Stuart, S. I. Nikolov, M. J. Pihl, Y. Du, J. H. Rasmussen, and M. F. Rasmussen, "SARUS: A synthetic aperture real-time ultrasound system," *IEEE Trans. Ultrason., Ferroelec., Freq. Contr.*, p. In press, 2013.
- [11] J. M. Hansen, M. C. Hemmsen, and J. A. Jensen, "An object-oriented multi-threaded software beamformation toolbox," in *Proc. SPIE Med. Imag.*, vol. 7968, March 2011, pp. 79680Y 1-9. [Online]. Available: <http://dx.doi.org/10.1117/12.878178>